Journal of Experimental Botany, Vol. 61, No. 12, pp. 3439–3449, 2010
doi:10.1093/jxb/erq168 Advance Access publication 17 June, 2010
This paper is available online free of all access charges (see http://jxb.oxfordjournals.org/open_access.html for further details)

Journal of Experimental Botany
www.jxb.oxfordjournals.org

RESEARCH PAPER

Development of synchronized, autonomous, and self-regulated oscillations in transpiration rate of a whole tomato plant under water stress

Rony Wallach[1,*], Noam Da-Costa[2], Michael Raviv[3] and Menachem Moshelion[2]

[1] The Seagram Center for Soil and Water Sciences, The Robert H Smith Faculty of Agriculture, Food and Environment, The Hebrew University of Jerusalem, PO Box 12, Rehovot 76100, Israel

[2] The Institute of Plant Sciences and Genetics in Agriculture, The Robert H Smith Faculty of Agriculture, Food and Environment, The Hebrew University of Jerusalem, PO Box 12, Rehovot 76100, Israel

[3] Department of Ornamental Horticulture, Agricultural Research Organization, Newe Ya'ar Research Center, PO Box 1021, Ramat Yishay 30095, Israel

* To whom correspondence should be addressed: E-mail: wallach@agri.huji.ac.il

Received 24 March 2010; Revised 18 May 2010; Accepted 20 May 2010

Abstract

Plants respond to many environmental changes by rapidly adjusting their hydraulic conductivity and transpiration rate, thereby optimizing water-use efficiency and preventing damage due to low water potential. A multiple-load-cell apparatus, time-series analysis of the measured data, and residual low-pass filtering methods were used to monitor continuously and analyse transpiration of potted tomato plants (*Solanum lycopersicum* cv. Ailsa Craig) grown in a temperature-controlled greenhouse during well-irrigated and drought periods. A time derivative of the filtered residual time series yielded oscillatory behaviour of the whole plant's transpiration (*WPT*) rate. A subsequent cross-correlation analysis between the *WPT* oscillatory pattern and wet-wick evaporation rates (vertical cotton fabric, 0.14 m^2 partly submerged in water in a container placed on an adjacent load cell) revealed that autonomous oscillations in *WPT* rate develop under a continuous increase in water stress, whereas these oscillations correspond with the fluctuations in evaporation rate when water is fully available. The relative amplitude of these autonomous oscillations increased with water stress as transpiration rate decreased. These results support the recent finding that an increase in xylem tension triggers hydraulic signals that spread instantaneously via the plant vascular system and control leaf conductance. The regulatory role of synchronized oscillations in *WPT* rate in eliminating critical xylem tension points and preventing embolism is discussed.

Key words: Embolism, hydraulic signal, oscillatory transpiration rate, plant–water relationship, whole-plant transpiration, xylem susceptibility.

Introduction

Stomata play a major role in water loss and carbon gain by regulating diffusive conductance in leaves. It is widely accepted that stomata respond to perturbations by many soil-plant-atmosphere signals but there is little agreement regarding the mechanism(s) by which they sense and react to such perturbations (Buckley, 2005).

The phenomenon of autonomous, cyclic opening and closing movements of stomata within a period of less than 3 h was observed over 40 years ago (Barrs, 1971). Those measurements showed that when the periodic variations in transpiration are plotted against time, a sine wave with a period of 10–90 min is obtained (Barrs and Klepper, 1968; Cox, 1968; Barrs, 1971; Teoh and Palmer, 1971). Such movements are most readily detected in a stable environment, but there seems to be no *a priori* reason why such movements cannot persist, albeit with

some modifications, in non-stable environments (Barrs, 1971).

Traditionally, two approaches have been taken to study the effect of environmental conditions on oscillatory transpiration. The first involves tracking the variations in transpiration rate of a small part of, or a whole leaf. The second focuses on the behaviour of individual stomata. Adopting the first approach, Ehrler *et al.* (1965), Barrs and Klepper (1968), Lang *et al.* (1969), Cardon *et al.* (1994), Naidoo and von Willert (1994), Herppich and von Willert (1995), Jarvis *et al.* (1999), and Prytz *et al.* (2003) studied oscillations in whole leaves from a large variety of species, most often using gas-exchange techniques. Measurements of chlorophyll *a* fluorescence (Siebke and Weis, 1995), leaf temperature or leaf water potential in terms of water relations (Ehrler *et al.*, 1965; Barrs and Klepper, 1968; Lang *et al.*, 1969; McBurney and Costigan, 1984; Naidoo and von Willert, 1994; Herppich and von Willert, 1995; Prytz *et al.*, 2003) have also been used to record stomatal oscillations. A common conclusion in all of these studies was that in-phase oscillations are induced by various agents, bringing about abrupt stomatal opening or closure. Reports of the synchronous rhythmic pattern of stomatal activity in different leaves on the same plant were reviewed by Hopmans (1969) and Lang *et al.* (1969). These authors found oscillations in leaf-xylem water potential and proposed that these are a necessary condition for the stomata of all leaves to oscillate in phase. Oscillations in root-xylem pressure were measured by Wegner and Zimmermann (1998) and Prytz *et al.* (2003), who noted that the synchronous behaviour observed during oscillatory transpiration indicates strong coupling among stomata; however, they did not suggest a coupling agent. Herppich and von Willert (1995) measured pronounced oscillations in stomatal apertures under certain climatic conditions and noted that changes in transpirational water loss during these oscillations are closely accompanied by changes in leaf water potential (Ψ_l).

On a stomatal scale, the simultaneous existence of different stomatal apertures, extents of stomatal opening across a leaf, and the possible implications of cross-CO_2 exchange were first discussed by Laisk and co-workers (Laisk *et al.*, 1980; Laisk, 1983). Terashima (1992) argued that under certain physiological conditions, the spatial distribution of different stomatal conductances is non-random (patchy), i.e. certain areas of a leaf can have a very different conductance from others. Patchy stomatal closure has been observed, particularly under water stress (Downton *et al.*, 1988; Beyschlag *et al.*, 1992) and low humidity (Mott and Parkhurst, 1991; Mott *et al.*, 1993, 1999), and following abscisic acid application (Daley *et al.*, 1989; Terashima, 1992; Mott, 1995).

Several models of the mechanism responsible for the oscillations in stomata aperture have been described (Lang *et al.*, 1969; Raschke, 1970; Cowan, 1972; Cardon *et al.*, 1994; Haefner *et al.*, 1997; McAinsh *et al.*, 1997; Shabala *et al.*, 1997; Meleshchenko, 2000; Bohn *et al.*, 2001), presenting a common basic assumption: that the oscillation behaviour is part of a feedback loop in which evaporation rate influences the stomatal aperture which, in turn, affects evaporation rate. Some have suggested that stomatal cycling is induced by internal fluctuations in water potential and flow resistance within the plant (Steudle, 2000).

Despite the fact that oscillations have been intensively studied in single stomata, leaf patches and whole leaves, oscillations on a whole-plant scale have been rather neglected. The studies of Rose and co-authors (Rose and Rose, 1994; Rose *et al.*, 1994) and Steppe *et al.* (2006) are, to the best of our knowledge, the only ones in which oscillations in whole-plant transpiration (*WPT*) have been measured. A recent study, which revealed that the long-distance signal triggering the reduction in leaf conductance under water stress is hydraulic rather than root-produced abscisic acid (Christmann *et al.*, 2007), led us to hypothesize that synchronized stomatal activity at the whole-plant level could be the result of a hydraulic signal spreading rapidly via the plant's vascular system. Consequently, this study aimed to isolate and characterize the autonomous, self-regulated oscillations in *WPT* rate that develop with increasing water stress.

Materials and methods

Experimental set-up

The experimental study was conducted in greenhouses at the Faculty of Agriculture, Food and Environment in Rehovot, Israel. The experimental set-up included 3.9 l growing pots placed on temperature-compensated load cells (Tadea-Huntleigh, Natanya, Israel) connected to a CR10 data logger (Campbell Scientific Inc., Logan, UT). The pots were filled with a commercial growing medium (a mixture of peat and tuff scoria) and each contained one plant. Each pot was immersed in a plastic container (13×21.5×31.5 cm, H×W×L) through a hole in its top cover. The pot tops and containers were sealed with aluminium foil to prevent evaporation. The well-irrigated treatment included daily filling of the container. The water level fell to 2 cm above the pot base after the irrigation events due to a drainage hole in the container side wall. The excess irrigation was intended to leach salts accumulated daily in the growth media. The pot-container system ensured that water was available to the plant throughout the day following irrigation, without supplemental irrigation. A commercial fertilizer solution ('Super Grow' 6-6-6+3 Hortical, Kadima, Israel) was added at 0.2% (v/v) daily with the irrigation water (fertigation). This set-up ensured that (i) the plants would not be subjected to water stress throughout the following day, and (ii) the container weight on the following day would decrease monotonically solely due to plant transpiration.

Tomato plants (*Solanum lycopersicum* cv. Ailsa Craig, previously known as *Lycopersicon esculentum* cv. Ailsa Craig) were grown in a controlled-environment greenhouse, with the temperature set at 18 °C during the night and 35 °C during the midday hours with periods of gradual variation between them. The effect of water stress on the patterns of *WPT*-rate oscillations was studied in a dehydration experiment using the tomato plants (at the age of 10–12 weeks). The plants were dehydrated by stopping irrigation, removing the containers in which the pots were immersed and allowing the plant to deplete the water from the growth medium in the pot for five successive days.

Average and momentary changes in atmospheric demand were assessed by measuring the weight loss from a vertical woven floor rag (0.14 m^2), the lower part of which was submerged in water in a container (noted hereafter as wet wick) that was placed on a load

cell. To isolate intrinsic noise associated with the 'measuring and data-acquisition systems' from the short-term fluctuations in plant transpiration, a constant load of ~6 kg (typical of the container+pot+plant weight) was placed on the load cells in the greenhouse for several days, during which the weight variation was monitored. The data from the load cells with plants, wet wick and constant load were analysed by the following time-series analysis.

Weight readings were taken every 10 s. The load-cell reading stabilized after 2 s following stimulation by dropping a 70-g steel ball from a height of 700 mm (manufacturer's data). Thus, a 10 s weight-sampling interval ensured that the maximum rate of weight decrease (0.5 g per 10 s) was appropriately followed. The data analysis consisted of two steps: the first included averaging 10 s readings over 3 min periods. This stage was aimed at decreasing the number of data points in further data analysis (second stage). The 3 min periods are clearly lower than the oscillation frequency (20–40 min) and higher than the Nyquist frequency (the highest frequency at which meaningful information can be obtained from a set of data). Skipping the first step had no effect on the outcome of the second stage.

Leaf areas were measured at the end of each experiment. Leaves were excised from each plant separately and their areas were measured using a leaf area scanner (Licor 3210, Lincoln, NE).

Data analysis

The rate of water loss from the system, being the negative value of the *WPT* rate, was calculated by the first derivative of the measured weight time series

$$WPT \equiv -\frac{dW}{dt} \approx \frac{W_{k+1} - W_k}{t_{k+1} - t_k} \quad (1)$$

where W_k and W_{k+1} are, respectively, the measured weights at time t_k and the following time step t_{k+1} In general, differentiation acts as a high-pass filter, thereby significantly amplifying the high-frequency noise, and noises are amplified as the measurement (sampling) interval (t_{k+1}–t_k, equation 1) decreases. Consequently, a signal treatment is essential when the noise associated with the transpiration-induced weight decrease is differentiated together with the high-frequency noises associated with the load-cell and data-acquisition systems, as both are embedded in the measured time series, owing to amplification of the noise introduced by the latter. In fact, measurement errors, which can never be avoided, complicate the differentiation, because these amplify the noise to such an extent that additional signal treatment is essential. The noise associated with the differentiation of noisy signals has stimulated a large number of investigations which have led to several solutions, in both the time and frequency domains (Savitzky and Golay, 1964; Cullum, 1971; Anderssen and Bloomfield, 1974*a*, *b*; Wahba, 1975; Rice and Rosenblatt, 1983; Scott and Scott, 1989).

Noise can be reduced or eliminated by smoothing (detrending) the measured data (time series) so that the smoothed data becomes stationary prior to the subsequent stage of spectral analysis. Many methods are used for smoothing noisy data in time-series analyses (Harvey and Shephard, 1993). These methods can be categorized as non-parametric smoothing [e.g. moving average, Savitzky-Golay (S-G), and Fast Fourier Transform (FFT) filtering] and non-parametric regression (fitting polynomials of various orders, exponential functions, symmetrical and asymmetrical-transition functions, etc to the measured data]. Smoothing should be performed with care since substantially different results can be obtained after differentiation, despite the high R^2 values that are usually obtained for the different smoothing methods. The Savitzky and Golay (1964) method (S-G) was used in this study to smooth the measured time series. This smoothing method is based on least-squares quadratic polynomial fitting (although higher orders can also be used) across a moving window within the data (Press *et al.*, 1988). The S-G method can be applied for various breadths of filtering windows, and it is considered a very good way of producing accurate smooth derivatives. The fit improves and includes fluctuations of higher frequencies and amplitudes with decreasing breadth of the filtering window. S-G with 30 data points was ultimately chosen for the window breadth as its time derivative provided a smooth (but not too smooth) pattern.

It is assumed herein that the container weight-time series follows an additive model

$$W_k = W(t_k) + \varepsilon_k, \quad 1 \leq k \leq n \quad t_1 < t_2 < \cdots t_k \cdots < t_n \quad (2)$$

where W is the value that the weight at time t_k would have if it varied smoothly with time, and ε_k is the deviation from that value. The system's weight oscillations superimposed on the smoothed time series also constitute a time series, designated 'residual time series' (residuals are the differences between the measured data and the fitted curve). When the mean of the residual time series is zero, the trend of the measured time series has been properly removed. The residual time series ε_k (equation 2) is a superposition of two time series: one made up of residuals that originate from the noises related to data acquisition, and the other of residuals originating from either the ambient conditions and/or the intrinsic oscillations in *WPT*. The time series for the constant-weight, wet-wick, and whole-plant runs (which were independently measured) were used to examine its randomness (white noise). The randomness of the noise originated from the data-acquisition system and the repeating patterns (periodicity) in the wet-wick and plant oscillations were examined by the autocorrelation function. This is a mathematical tool for finding repeating patterns, such as the presence of a periodic signal which has been buried under the noise function, by expressing the similarity between observations as a function of the time separation between them. If the noise is a white noise, the autocorrelation function should be near zero for any and all time-lag separations. If not a white noise, then one or more (except at lag=0) of the autocorrelations will be significantly non-zero.

The spectrum analysis of ε_k was used to explore the existence of cyclical patterns by decomposing the complex time series with cyclical components into a few underlying sinusoidal (sine and cosine) functions of particular wavelengths. The characteristics of the phenomenon of interest become apparent when the important underlying cyclical components are identified. The spectrum analysis enabled us to uncover a few cycles of different lengths in the time series of interest, which at first looked more or less like random noise.

The spectrum (amplitudes versus frequencies) of the residual time series was calculated by fast Fourier transform (FFT), which decomposes a time-domain signal or time series into complex exponentials (sines and cosines). The spectrum of the constant-load residual time series was used to determine the frequency threshold that would be used to filter out the high-frequency noise (low-pass filter) from the plant-weight residual time series. Subsequently, the filtered spectrum was reconstructed back to a time series (in the time domain) by inverse FFT. The calculations of the above were executed by TableCurve 2D® (Systat Software Inc, CA). The time derivative of the reconstructed low-pass-filtered time series $d(\varepsilon_k')/dt$ ((ε_k') is the low-pass filter of ε_k) provided the oscillatory transpiration rate that superimposes the smoothed *WPT* rate.

The evaporation rate (smoothed and oscillatory) from the wet wick integrates the effect of the ambient conditions on both the wick and the plant. A high correlation between the two time series is expected under optimal growth conditions, while deviations are likely to occur when the plants are exposed to stresses. The wet-wick evaporation rate-time series is regarded as the input to the plant system and the *WPT* rate-time series as the output. Hence, a comparison between the patterns of smoothed and low-pass oscillations in *WPT* rate and wet-wick evaporation rate can reveal whether the synchronized oscillations in *WPT* rate are mainly driven by fluctuations in ambient conditions in the greenhouse, or if they tend to become autonomous under certain independent

conditions (e.g. water stress). The relationship between the two time series can be interpreted by quantitative and qualitative means. A qualitative estimation of the correlation between the transpiration- and evaporation-rate time series can be obtained by plotting the two time series on the same plot and a quantitative estimation is obtained by the cross-correlation function. A plot of the time series enables isolating periods throughout the day during which the two time series deviate, and relating these periods to the variation of the smoothed patterns of these variables or to other independent variables in the system. A cross-correlation function with a single and pronounced peak indicates that the transpiration and wet-wick evaporation oscillatory patterns are related, and that the oscillatory *WPT* rate is driven by the fluctuations in ambient conditions (evaporative demand). A peak value close to 1 located at lag=0 indicates that the changes in *WPT* rate are fully and instantaneously driven by the fluctuations in evaporative demand, as reflected by the wet wick. As the *WPT* rate of a well-watered plant responds to environmental conditions, a good correlation coefficient is expected between well-watered plants and the wet wick, the latter closely simulating the evaporative demand. However, a perfect correlation coefficient was not anticipated as the boundary-layer resistances between the wet wick and the plant crown are dissimilar, the thermal properties and heat capacity of the two systems differ, and the plant can control its diffusive resistance by changing stomatal aperture. On the other hand, a rippled, low-value cross-correlation function, with no clear peak, can be interpreted as a lack of dependence between the two time series, namely, the oscillations in *WPT* rate are autonomous and self-regulated, independent of the fluctuations in ambient conditions.

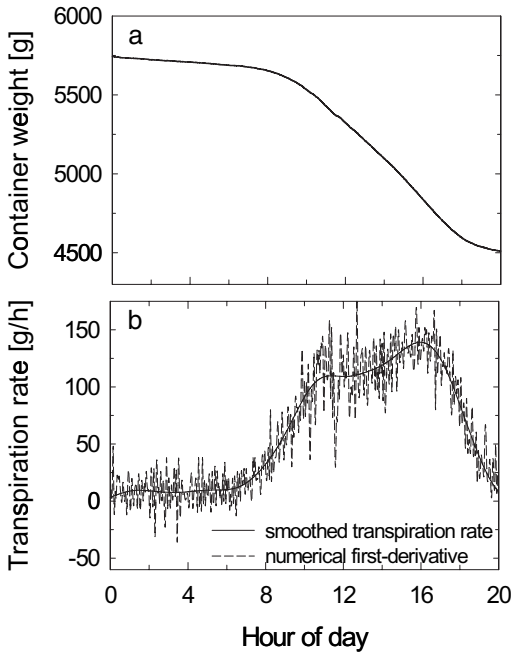

Fig. 1. Time-course of changing weight of a potted tomato plant (a). Time-course of transpiration rate calculated by numerical derivative of the measured and smoothed time-courses of the decrease in potted tomato weight (b).

Results

Oscillations in WPT *rate*

Typical variations in weight during the night and subsequent daylight hours are shown in Fig. 1a for a tomato plant grown under ample water supply. As water was supplied to the plants in the late evening (after 20.00 h), the weight decreased monotonically, albeit at different rates, during the night and daylight hours. The rate of the weight decrease (transpiration rate increase) intensified during the morning, stayed high during the noon and early afternoon hours, and weakened thereafter (Fig. 1b). The *WPT*-rate time series (the negative values of the rate of weight decrease), calculated by the time derivative of the measured weight-time series with data points every 3 min (equation 1), is shown in Fig. 1b (dashed line). A noisy *WPT* rate was obtained despite what appeared to be a relatively smooth pattern of weight decrease (Fig. 1a). The amplitudes of the *WPT* rate were low during the night, early morning, and evening hours and large at the other times. A detailed pattern of the daily transpiration rate, especially when the ambient conditions varied with time, could barely be identified from this noisy time series. The smoothed *WPT* rate (Fig. 1b, solid line) was obtained by differentiating a smoothed weight-time series obtained by applying the S-G smoothing method with a window breadth of 30 data points (S-G 30). The fluctuations around the smoothed transpiration-rate pattern are usually considered random noise (white noise) associated with the measurement system, and as such are generally ignored without further analysis. Here, however, these fluctuations were further analysed in order to isolate the system-noise-induced fluctuations from those induced by the ambient and/or physiologically driven oscillations.

The smoothed patterns of weight-variation rate (smoothed by S-G 30 prior to time differentiation) for a tomato plant, a wet wick, and a constant weight that was placed on a load cell are shown in Fig. 2a, b, c, respectively. The whole-plant and wet-wick data were measured on 6 September 2006, and the constant load on 9 September 2006, all in the temperature-controlled greenhouse. Patterns similar to the one shown in Fig. 2a were measured for four neighbouring tomato plants that were grown together in the greenhouse (data not shown) with a similarly ample water supply. The residual time series (difference between the measured and smoothed weight time series) for the tomato plant, wet wick, and constant load are shown in Fig. 2d, e, f, respectively. To exclude the possibility of the oscillations in *WPT* rate being simply system-related noise, these residuals were examined for randomness (white noise) by autocorrelation function (Fig. 2g, h, i, respectively). The autocorrelation function of the constant-weight residual time series, ε_k (Fig. 2i) was 1 at lag=0 and was close to zero for all other lags. Note that one lag represents 3 min. This autocorrelation function shape indicated that ε_k is indeed white noise. By contrast, the autocorrelation functions of both the tomato plant and the wet wick (Fig. 2g, h, respectively) were periodic for the first 200 lags, with an approximate average 40 lag difference from peak to peak. The correlation between the fluctuations in plant weight around the smoothed weight variation and ambient

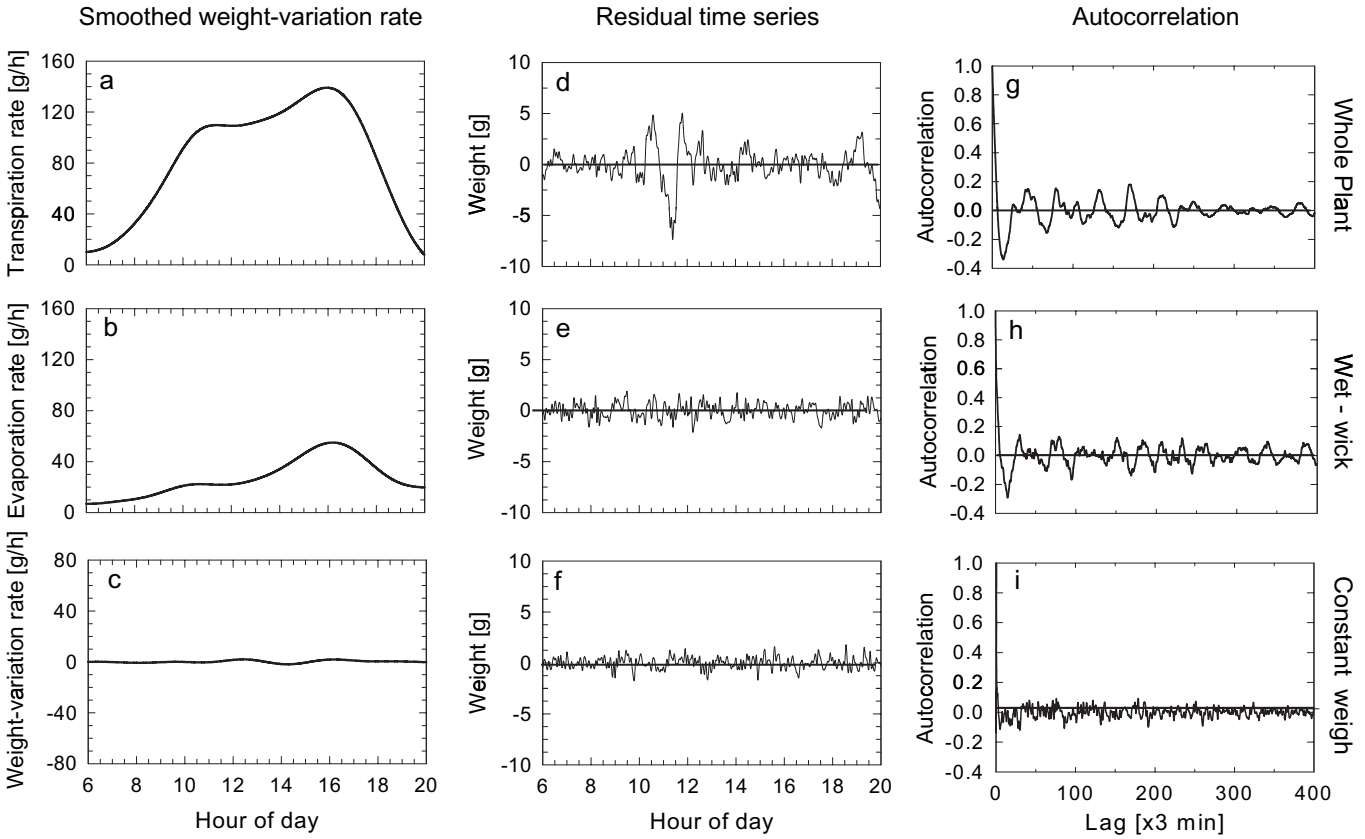

Fig. 2. Smoothed weight-variation-rate patterns in a whole potted tomato plant (a), a wet wick (b), and a constant load (c). Residual time series for the whole plant (d), wet wick (e), and constant load (f). Autocorrelation function of the residual time series for the whole plant (g), wet wick (h), and constant load (i).

conditions (represented by the wet wick) will be analysed further in the following.

The spectra for the tomato-plant, wet-wick, and constant-load residual time series are shown in Fig. 3a, c, e, respectively. The overall flat spectrum of the constant load (Fig. 3e) provided an additional indication that its residual time series is practically a random signal (white noise) while those of the plant and wet wick are not. The spectrum for the tomato plant (Fig. 3a) had high amplitudes at f <2.5 h^{-1} and lower amplitudes at the higher frequencies. The wet-wick spectrum (Fig. 3c) exhibited a similar pattern, i.e. high amplitudes (although lower than those of the whole plant) at f <2 h^{-1} and lower amplitudes at the higher frequencies. To filter out what was considered to be white noise, both spectra were low-pass filtered for f <2 h^{-1} prior to further analysis. The time derivative of the reconstructed low-pass-filtered residual time series provided oscillations in *WPT* and wet-wick evaporation rates, as well as in the constant-load weight. Superpositions of these oscillations on the smoothed variation of these variables are shown in Fig. 3b, d, f, respectively.

To analyse the correlation between the fluctuations in *WPT* and wet-wick rates, the time derivatives of the reconstructed low-pass-filtered residual time series of these variables were plotted together in Fig. 4a. The baseline in this figure (weight loss=0) was the smoothed transpiration/evaporation rate. The plant's oscillatory transpiration and wet-wick evaporation in Fig. 4a appeared to be correlated. A quantitative measure of this correlation was obtained by the cross-correlation function (Fig. 4b), which is a standard method of estimating the degree to which two series are correlated. The cross-correlation between the two series was calculated for the morning (06.00 to 12.00 h) and afternoon (12.00 to 18.00 h) to examine the correlation between fluctuations in ambient conditions and the oscillations in *WPT* rate when transpiration rate increases (morning hours) and when it is already high and beginning to decrease (afternoon hours). When the cross-correlation around lag=0 is higher than those at other lag values (negative and positive), the oscillations in *WPT* rate can be more related to temporary variations (fluctuations) in ambient conditions. However, when low cross-correlation values are obtained at all lags, the two series are independent and the oscillations in *WPT* rate may be autonomous, putatively driven by independent physiological processes. The cross-correlation function for the morning hours had a slightly higher peak value than for the afternoon hours (Fig. 4b), but neither had only one single peak. The presence of multiple peaks indicated that the oscillations in *WPT* rate depend on the fluctuations in ambient conditions, with periods when the oscillations in *WPT* rate are independent of those of the wet wick, namely, ambient conditions. A careful consideration of the patterns of transpiration and evaporation oscillations (Fig. 4a)

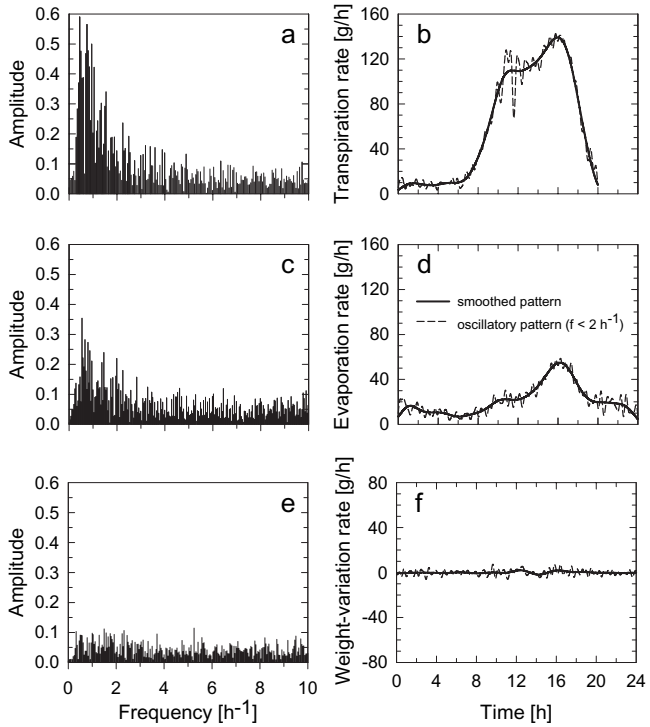

Fig. 3. Spectra for the whole-plant (a), wet-wick (b), and constant-load (c) residual time series. Time derivative of the low-pass-filtered residual time series superimposed on the time derivative of the smoothed weight variation with time for the whole plant (d), wet wick (e), and constant load (f).

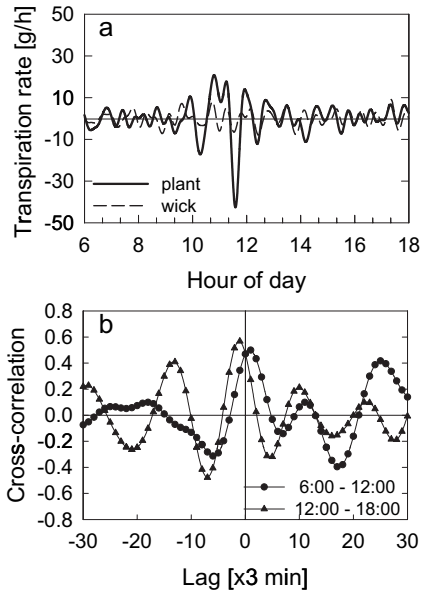

Fig. 4. Oscillations in whole-plant transpiration (*WPT*) and wet-wick evaporation rates superimposed on the smoothed rates when the low-pass-filtered data are used to derive the transpiration and evaporation rates (a). Cross-correlation function between transpiration and evaporation rates in the morning and afternoon hours (b). One lag represents 3 min.

revealed that they are temporarily out of phase between 07.30 and 10.00 h and between 13.30 and 15.30 h. From the smoothed transpiration pattern in Fig. 3b, the shifts between the two oscillations coincided with periods of intensive change in transpiration rate—be it increasing or decreasing. Thus, it may be deduced that autonomous oscillations in *WPT* rate are associated with intensive variations in transpiration rate, even when water is fully available to the plant.

The effect of water stress on the pattern of oscillations in WPT *rate*

The effect of water-stress build-up on the momentary *WPT* rate (smoothed and oscillatory) is shown in Fig. 5a for plant I, and in Fig. 5c for plant II. The difference between the smoothed and oscillatory *WPT* rates in Fig. 5a and c is shown in Fig. 5b and 5d, respectively, where the value of zero transpiration rate represents the smoothed transpiration rate in Fig. 5a and 5c, used as a reference. The last irrigation took place on the evening preceding the first day in Fig. 5. The containers in which the pots were immersed were removed after this irrigation. The smoothed and superimposed oscillatory evaporation rates from the wet wick for the 5 d dehydration period are shown in Fig. 5e and the isolated oscillations in evaporation rate (the difference between the smoothed and oscillatory patterns) for this period are shown in Fig. 5f. Figure 5 indicates that (i) Since these plants were grown in a temperature-controlled greenhouse with a repetitive pattern of daily ambient conditions (demonstrated by the repetitive daily pattern in wet-wick evaporation rate, Fig 5e), water can be assumed to be fully available to the plant as long as the transpiration-rate pattern is similar to the previous day. Accordingly, water seems to be fully available to plant I during the first 2 d of dehydration, and to plant II only on the first day (Fig. 5a, c, respectively). As opposed to plant I, whose transpiration rate decreased slightly on days 2 and 3 and substantially on days 4 and 5, the transpiration rate of plant II decreased substantially on day 2 and was markedly low during the last 3 d of dehydration. Differences in size between the two plants led to a significant difference in the maximum transpiration rate on day 1 (90 g h^{-1} versus 160 g h^{-1} for plants I and II, respectively) and the amount of water remaining in the pots. (ii) Similar to the transpiration-rate pattern in Fig. 2a, the smoothed transpiration-rate patterns in Fig. 5a and c have two daily peaks: a lower peak at noon followed by a higher one in the afternoon. Note that the timing of the second daily peak coincides with the peak in daily evaporation rate. The two peaks in transpiration rate occurred despite the single daily peak in evaporation rate (Fig. 5e). Furthermore, the two peaks in transpiration rate were accompanied by a change in the pattern of transpiration-rate oscillations: the oscillations were amplified while the transpiration rate increased toward the first and even the second peak, and were shifted from their concurrence with the oscillations in evaporation rate (Figs 2a, 5a–d). The increase in oscillation amplitude during this period contrasted with the uniform distribution of oscillation amplitudes in evaporation rate (Fig. 5f).

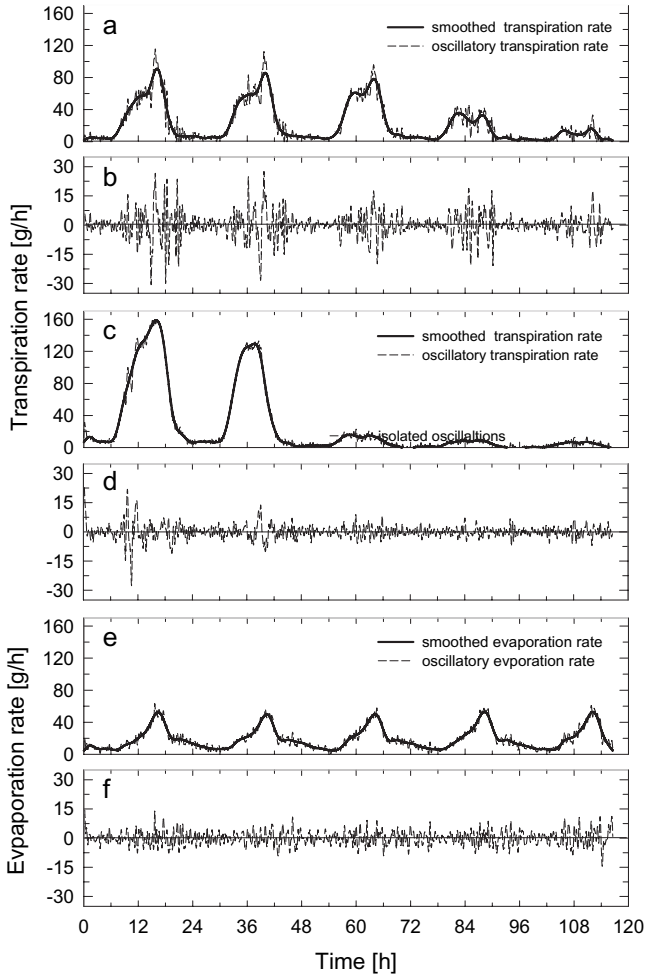

Fig. 5. Smoothed and oscillatory whole-plant transpiration (*WPT*) rate for tomato plant I (a), isolated oscillations in *WPT* rate for tomato plant I (b), smoothed and oscillatory *WPT* rate for tomato plant II (c), isolated oscillations in *WPT* rate for tomato plant II (d), smoothed and superimposed oscillatory evaporation rates from the wet wick (e), and isolated oscillations in wet-wick evaporation rate (f), for five continuous days of dehydration.

(iii) The ratio between the values of the two daily transpiration-rate peaks diminished with increasing water stress and was associated with the formation of a noticeable dip between the two peaks. (iv) The increase in oscillation amplitudes that was associated with transpiration-rate variation (increase in the morning hours or decrease in the afternoon hours) during the early stages of dehydration (Fig. 5a, c) was also seen in the dip between the two daily transpiration-rate peaks as water stress progressed.

The oscillation amplitudes relative to the transpiration/evaporation rate (hereafter designated relative oscillations) are shown in Fig. 6 for the first and fourth days of dehydration. The relative oscillations are the ratio between the isolated oscillations in transpiration/evaporation rate and the smoothed transpiration/evaporation rate, respectively, in Fig. 5. The relative oscillations in evaporation rate are larger in the early morning hours when the evaporation rate is low (Fig. 5e), and then decrease as the evaporation rate increases and increase again in the late afternoon hours when the evaporation rate decreases again (Fig. 6e, f). Figure 6a–d shows that the relative oscillations in transpiration increase during the dehydration period together with the decrease in transpiration rate (Fig. 5a, c). The oscillations in *WPT* rate may be temporary, and even decrease to zero (Relative Transpiration= –1 in Fig. 6b) under severe drought conditions when the transpiration rate is low. The daily pattern of relative oscillations in transpiration rate during the advanced dehydration stages (e.g. Fig. 6b, d) indicates that they are relatively low in the morning, then intensify and stay high, even in the late afternoon hours.

A comparison between the daily isolated oscillations in transpiration and wet-wick evaporation rates for dehydrating tomato plants I, together with the cross-correlation function for each dehydration day, are shown in Fig. 7. The cross-correlation function for each dehydration day for plant II is shown (hollow circles) in Fig. 7b, d, f, h, and j as well. The cross-correlation function for plant I had an apparent single peak on day 1 (Fig. 7b), when water was still fully available. This high cross-correlation value indicates that the synchronized oscillations in *WPT* rate were mostly induced by the fluctuations in ambient conditions in the greenhouse. However, there were no evident peaks in the cross-correlation function as water stress increased, which indicates that the synchronized oscillations in transpiration rate became self-regulated and independent of the fluctuations in ambient conditions demonstrated by the pattern of wet-wick evaporation. The decrease in transpiration rate along with the development of self-regulated oscillations in transpiration rate took place while the gap between water demand and water availability broadened. Note that the self-regulated oscillations in plant I appeared on days 2 and 3 of dehydration (Fig. 7d, f), while the transpiration rates were similar to that on day 1 (Fig. 5a). By contrast, the daily cross-correlation function for plant II did not have any apparent single peak, not even on day 1 (the hollow circles in Fig. 7b). The differences in the cross-correlation functions between the two plants can be attributed to the high transpiration rate of plant II on day 1 (Fig. 5c), which was probably accompanied by stress-induced behaviour. Plant II was 6% heavier and had 7% higher leaf area than plant I.

Discussion

The development of autonomous and self-regulated oscillations in *WPT* rate is postulated to be the plant response to the increasing gap between the evaporative demand and water availability. Although the relative oscillations increased as water stress intensified (Fig. 6a–d), their short-term variation was associated with the temporal variations in the between evaporative-demand to water-availability balance. The relative oscillations were low during the early morning hours, then increased with the increase in evaporative demand, and remained high during the afternoon hours when the evaporative demand had already decreased

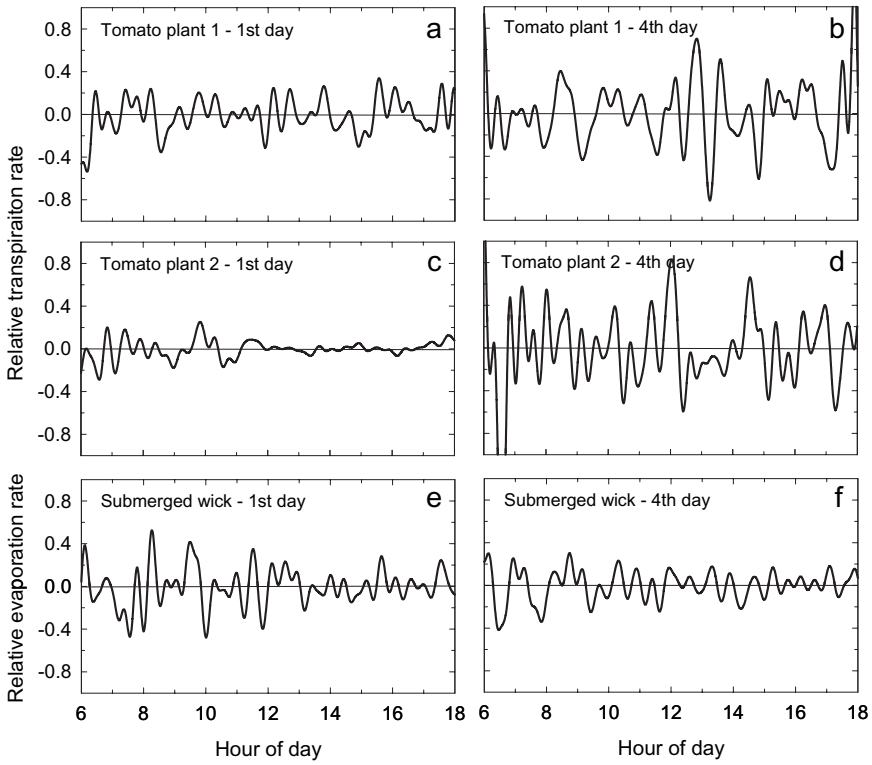

Fig. 6. Isolated oscillations in whole-plant transpiration (*WPT*) rate relative to the momentary values of the smoothed *WPT* rate for: plant I on day 1 (a) and day 4 (b) of dehydration, plant II on day 1 (c) and day 4 (d) of dehydration. Isolated oscillations in evaporation rate relative to the momentary values of the smoothed evaporation rate from the wet wick for day 1 (e) and day 4 (f) of dehydration.

(Fig. 6b, d). Given that transpiration rate is highly dependent on temporal variation in soil water content (Kramer and Boyer, 1995; Ray and Sinclair, 1998; Doussan *et al.*, 2006; Garrigues *et al.*, 2006), the following scenario can be hypothesized to explain this irregular pattern of the relative oscillations. The moisture content around the plant root is usually lower at the end of the day and is gradually replenished during the night by mass flow from the wetter soil bulk. When the moisture content in the soil is high, this water flow from the bulk soil to the root vicinity also takes place during the daylight hours at a rate that enables the plant to catch up with the evaporative demand (first 2 d in Fig. 5a). When the transpiration rate follows the evaporative demand, soil water is considered fully available at the given evaporative demand. However, when soil water becomes depleted, the flow rate from the soil bulk to the root vicinity decreases owing to an increase in the soil's resistance to flow, and the transpiration rate decreases despite the high evaporative demand (last 3 d in Fig. 5a and last 4 d in Fig. 7a). When the soil becomes dry, the only available water that can cope with the evaporative demand is the amount around the roots in the morning hours when the replenished water there can handle the concurrent low evaporative demand. Therefore, the relative oscillations are low during this period (Fig. 6b, d). However, when the evaporative demand increases and water content in the root vicinity is nearly depleted with no replenishment from the soil bulk, the relative oscillation amplitudes intensify with decreasing transpiration rate (Fig. 6b, d).

Plants are exposed to the risk of embolism under high evaporative demand, and particularly under drought stress owing to the increase in xylem tension, which is generally seen as a potentially catastrophic dysfunction of the axial water-conducting system (Tyree and Sperry, 1989; Tardieu and Davies, 1993; Hacke and Sauter, 1995). One interpretation of the observations in this study is that the autonomous and self-regulated oscillations in *WPT* rate with higher relative amplitudes are designed to diminish or even prevent the increase in xylem tension. Support for this interpretation can be found in the study by Qiu *et al.* (2002) in which the relationship between acoustic emission, transpiration rate, and water stress in tomato plants was measured. Qiu *et al.* (2002) reported that under mild or no conditions of water stress, the acoustic emission (representing the development of embolism) significantly increases with transpiration rate, both positively and negatively. This observation agrees with our finding that temporary autonomous oscillations in *WPT* rate develop when the transpiration rate is sharply increasing in the morning hours (and sharply decreasing in the afternoon) (Figs 4a, 7a). In addition, Qiu *et al.* (2002) showed that the acoustic emission increases with a decrease in the amount of soil water under mild or moderate conditions of water stress, and decreases with the decrease in the amount of soil water under severe water stress. Other studies revealing a link between stomatal conductance, leaf water potential, and xylem embolism were performed by Salleo *et al.* (2000) and Sperry (2000). They suggested that xylem embolism may be a pre-signal for

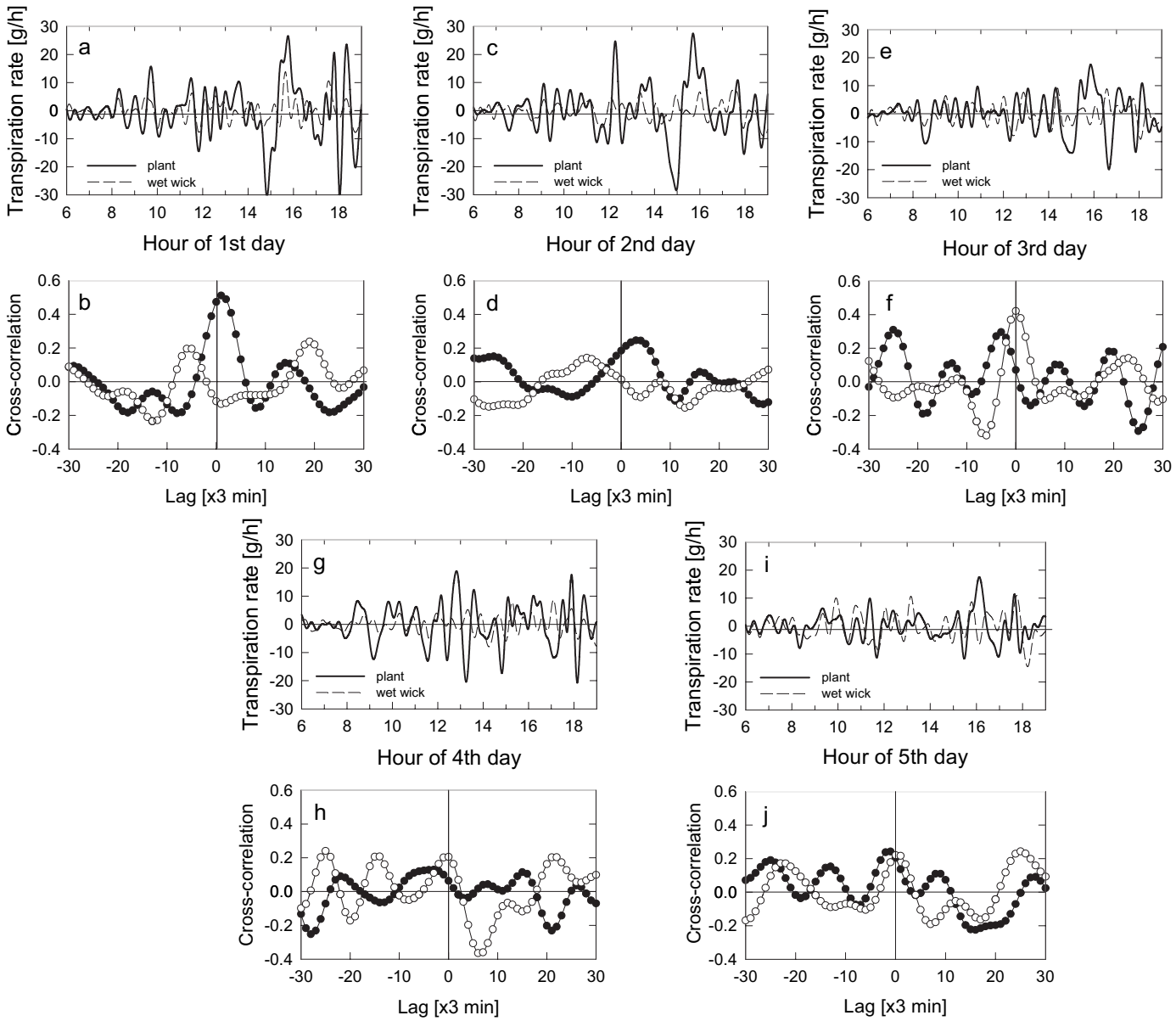

Fig. 7. Comparison between the isolated oscillations in tomato plant I transpiration and wet-wick evaporation rates and the respective cross-correlation function for these oscillations (filled circles) during the 5 d dehydration experiment: day 1 (a and b, respectively), day 2 (c and d, respectively), day 3 (e and f, respectively), day 4 (g and h, respectively), day 5 (i and j, respectively). The cross-correlation function for plant II during the 5 d dehydration experiment appear in b, d, f, h, and j, respectively as hollow circles.

stomatal closure, thus representing an important step in the stomatal control of transpiration. The important role of the long (root-to-shoot) hydraulic signal in inducing stomatal closure under water stress has recently been reported (Christmann *et al.*, 2007).

The independent findings of a correlation between water stress and the formation of cavitation (Salleo *et al.*, 2000; Qiu *et al.*, 2002; and others) and the development of autonomous self-regulated oscillations in *WPT* rate under water stress suggest that these oscillations are related to the plant's response to increasing xylem tension. Consequently, it is postulated that the oscillations in *WPT* rate are driven by a rapid, root-induced hydraulic signal that spreads instantaneously throughout the entire vascular system and *inter alia*, regulates stomatal aperture.

Could the oscillations in *WPT* rate be related to short-term growth of the plant? Tomato plants maintain almost constant weight during the day, while their growth periods take place from the late afternoon to early morning (Menzel *et al.*, 2009). Tomato plants present ishohdric behaviour (Sade *et al.*, 2009), namely, maintaining constant leaf relative water content during midday, under high available water conditions and drought condition alike. Combining this intrinsic property with the observations that the autonomous and self-regulated oscillations in *WPT* appeared only under water stress, suggest that the measured oscillations were not induced by short-term oscillations in the plant's growth.

In conclusion, synchronized autonomous self-regulated oscillations in *WPT* rate with periods of 20–50 min were

measured for tomato plants under water stress. These oscillations were interpreted as changes in leaf conductance triggered by hydraulic signals spread instantaneously via the plant vascular system which resulted from drought-induced xylem tension. Though the role of the oscillations is not yet clear, a plausible assumption is that they are a means used by the plant to control xylem tension while preventing the critical tension threshold that impels embolism.

Acknowledgement

This work was partially supported by a grant (no. 904-4.12/06) from the German-Israeli Foundation for Scientific Research and Development (GIF).

References

Anderssen RS, Bloomfield P. 1974*a*. Numerical differentiation procedures for non exact data. *Numerische Mathematik* **22,** 157–182.

Anderssen RS, Bloomfield P. 1974*b*. Time series approach to numerical differentiation. *Technometrics* **16,** 69–75.

Barrs HD. 1971. Cyclic variations in stomatal aperture, transpiration, and leaf water potential under constant environmental conditions. *Annual Review of Plant Physiology* **22,** 223–236.

Barrs HD, Klepper B. 1968. Cyclic variations in plant properties under constant environmental conditions. *Physiologia Plantarum* **21,** 711–730.

Beyschlag W, Pfanz H, Ryel RJ. 1992. Stomatal patchiness in Mediterranean evergreen sclerophylls: phenomenology and consequences for the interpretation of the midday depression in photosynthesis and transpiration. *Planta* **187,** 546–553.

Bohn A, Geist A, Rascher U, Luttge U. 2001. Responses to different external light rhythms by the circadian rhythm of crassulacean acid metabolism in kalanchoe daigremontiana. *Plant, Cell and Environment* **24,** 811–820.

Buckley TN. 2005. The control of stomata by water balance. *New Phytologist* **1682,** 275–291.

Cardon ZG, Berry JA, Woodrow IE. 1994. Dependence of the extent and direction of average stomatal response in *Zea mays* L. and *Phaseolus vulgaris* L. on the frequency of fluctuations in environmental stimuli. *Plant Physiology* **105,** 1007–1013.

Christmann A, Weiler EW, Steudle E, Grill E. 2007. A hydraulic signal in root-to-shoot signalling of water shortage. *The Plant Journal* **52,** 167–174.

Cowan IR. 1972. Oscillations in stomatal conductance and plant functioning associated with stomatal conductance: observations and a model. *Planta* **106,** 185–219.

Cox EF. 1968. Cyclic changes in transpiration of sunflower leaves in a steady environment. *Journal of Experimental Botany* **19,** 167–175.

Cullum J. 1971. Numerical differentiation and regularization. *Siam Journal on Numerical Analysis* **8,** 254–265.

Daley PF, Raschke K, Ball JT, Berry JA. 1989. Topography of photosynthetic activity of leaves obtained from video images of chlorophyll fluorescence. *Plant Physiology* **90,** 1233–1238.

Doussan C, Pierret A, Garrigues E, Pagès C. 2006. Water uptake by plant roots: II. Modelling of water transfer in the soil–root system with explicit account of flow within the root system: comparison with experiments. *Plant and Soil* **283,** 99–117.

Downton WJS, Loveys BR, Grant WJR. 1988. Non-uniform stomatal closure induced by water-stress causes putative non-stomatal inhibition of photosynthesis. *New Phytologist* **110,** 503–509.

Ehrler WL, Nakayama FSV, Bavel CHM. 1965. Cyclic changes in water balance and transpiration of cotton leaves in a steady environment. *Physiologia Plantarum* **18,** 766–775.

Garrigues E, Doussan C, Pierret A. 2006. Water uptake by plant roots. I. Formation and propagation of a water extraction front in mature root systems as evidenced by 2D light transmission imaging. *Plant and Soil* **283,** 83–98.

Hacke U, Sauter JJ. 1995. Vulnerability of xylem to embolism in relation to leaf water potential and stomatal conductance in *Fagus sylvatica* f. *purpurea* and *Populus balsamifera*. *Journal of Experimental Botany* **46,** 1177–1183.

Haefner JW, Buckley TN, Mott KA. 1997. A spatially explicit model of patchy stomatal responses to humidity. *Plant, Cell and Environment* **20,** 1087–1097.

Harvey AC, Shephard N. 1993. Structural time series models. *Handbook of Statistics* **11,** 261–302.

Herppich WB, von Willert DJ. 1995. Dynamic changes in leaf bulk water relations during stomatal oscillations in mangrove species: continuous analysis using a dewpoint hygrometer. *Physiologia Plantarum* **94,** 479–485.

Hopmans PAM. 1969. Types of stomatal cycling and their water relations in bean leaves. *Zeitschrift für Pflanzenphysiologie* **60,** 242–254.

Jarvis AJ, Young PC, Taylor CJ, Davies WJ. 1999. An analysis of the dynamic response of stomatal conductance to a reduction in humidity over leaves of *Cedrella odorata*. *Plant, Cell and Environment* **22,** 913–924.

Kramer PJ, Boyer JS. 1995. *Water relations of plant and soils*. Orlando, FL: American Press.

Laisk A. 1983. Calculation of leaf photosynthetic parameters considering the statistical distribution of stomatal apertures. *Journal of Experimental Botany* **34,** 1627–1635.

Laisk A, Oja V, Kull K. 1980. Statistical distribution of stomatal apertures of *Vicia faba* and *Hordeum vulgare* and the *Spannungsphase* of stomatal opening. *Journal of Experimental Botany* **31,** 49–58.

Lang ARG, Klepper B, Cumming MJ. 1969. Leaf water balance during oscillation of stomatal aperature. *Plant Physiology* **44,** 826–830.

McAinsh MR, Brownlee C, Hetherington AM. 1997. Calcium ions as second messengers in guard cell signal transduction. *Physiologia Plantarum* **100,** 16–29.

McBurney T, Costigan PA. 1984. Rapid oscillations in plant water potential measured with a stem psychrometer. *Annals of Botany* **54,** 851–853.

Meleshchenko SN. 2000. Water-transport system and its components in higher plants. 5. Dynamic model of the water-transport

system in transpiring plants. *Russian Journal of Plant Physiology* **47,** 826–834.

Menzel MI, Tittmann S, Bühler J, *et al*. 2009. Non-invasive determination of plant biomass with microwave resonators. *Plant, Cell and Environment* **32,** 368–379.

Mott KA. 1995. Effects of patchy stomatal closure on gas-exchange measurements following abscisic-acid treatment. *Plant, Cell and Environment* **18,** 1291–1300.

Mott KA, Cardon ZG, Berry JA. 1993. Asymmetric patchy stomatal closure for the two surfaces of *Xanthium strumarium* L. leaves at low humidity. *Plant, Cell and Environment* **16,** 25–34.

Mott KA, Parkhurst DF. 1991. Stomatal responses to humidity in air and helox. *Plant, Cell and Environment* **14,** 509–515.

Mott KA, Shope JC, Buckley TN. 1999. Effects of humidity on light-induced stomatal opening: evidence for hydraulic coupling among stomata. *Journal of Experimental Botany* **50,** 1207–1213.

Naidoo G, von Willert DJ. 1994. Stomatal oscillations in the mangrove *Avicennia germinans*. *Functional Ecology* **8,** 651–657.

Press WH, Flannery BP, Teukolsky SA, Vetterling WT. 1988. *Numerical recipes in C: the art of scientific computing*. Cambridge, UK: Cambridge University Press.

Prytz G, Futsaether CM, Johnsson A. 2003. Thermography studies of the spatial and temporal variability in stomatal conductance of *Avena* leaves during stable and oscillatory transpiration. *New Phytologist* **158,** 249–258.

Qiu GY, Okushima L, Sase S, Lee IB. 2002. Acoustic emissions in tomato plants under water stress conditions. *Japan Agricultural Research Quarterly* **36,** 103–109.

Raschke K. 1970. Leaf hydraulic system. Rapid epidermal and stomatal responses to changes in water supply. *Science* **167,** 189–191.

Ray JD, Sinclair TS. 1998. The effect of pot size on growth and transpiration of maize and soybean during water deficit stress. *Journal of Experimental Botany* **49,** 1381–1386.

Rice J, Rosenblatt M. 1983. Smoothing splines: regression, derivatives and deconvolution. *Annals of Statistics* **11,** 141–156.

Rose MA, Beattie DJ, White JW. 1994. Oscillations of whole-plant transpiration in moonlight rose. *Journal of the American Society for Horticultural Science* **119,** 439–445.

Rose MA, Rose MA. 1994. Oscillatory transpiration may complicate stomatal conductance and gas-exchange measurements. *HortScience* **29,** 693–694.

Sade N, Vinocur BJ, Diber A, Shatil A, Ronen G, Nissan H, Wallach R, Karchi H, Moshelion M. 2009. Improving plant stress tolerance and yield production: is the tonoplast aquaporin SlTIP2;2 a key to isohydric to anisohydric conversion? *New Phytologist* **181,** 651–661.

Salleo S, Nardini A, Pitt F, Lo Gullo MA. 2000. Xylem cavitation and hydraulic control of stomatal conductance in laurel (*Laurus nobilis* L.). *Plant, Cell and Environment* **23,** 71–79.

Savitzky A, Golay MJE. 1964. Smoothing and differentiation of data by simplified least squares procedurs. *Analytical Chemistry* **36,** 1627–1639.

Scott LB, Scott LR. 1989. Efficient methods for data smoothing. *Siam Journal on Numerical Analysis* **26,** 681–692.

Siebke K, Weis E. 1995. Assimilation images of leaves of *Glechoma hederacea*: analysis of nonsynchronous stomata related oscillations. *Planta* **196,** 155–165.

Shabala SN, Newman IA, Morris J. 1997. Oscillations in H^+ and Ca^{2+} ion fluxes around the elongation region of corn roots and effects of external pH. *Plant Physiology* **113,** 111–118.

Sperry JS. 2000. Hydraulic constraints on plant gas exchange. *Agricultural and Forest Meteorology* **104,** 13–23.

Steppe K, Dzikiti S, Lemeur R, Milford JR. 2006. Stomatal oscillations in orange trees under natural climatic conditions. *Annals of Botany* **97,** 831–835.

Steudle E. 2000. Water uptake by roots: effects of water deficit. *Journal of Experimental Botany* **51,** 1531–1542.

Tardieu F, Davies WJ. 1993. Integration of hydraulic and chemical signaling in the control of stomatal conductance and water status of droughted plants. *Plant, Cell and Environment* **16,** 341.

Teoh CT, Palmer JH. 1971. Nonsynchronized oscillations in stomatal resistance among sclerophylls of *Eucalyptus umbra*. *Plant Physiology* **47,** 409–411.

Terashima I. 1992. Anatomy of nonuniform leaf photosynthesis. *Photosynthesis Research* **31,** 195–212.

Tyree MT, Sperry JS. 1989. Vulnerability of xylem to cavitation and embolism. *Annual Review of Plant Physiology and Plant Molecular Biology* **40,** 19–38.

Wahba G. 1975. Smoothing noisy data with spline functions. *Numerische Mathematik* **24,** 383–393.

Wegner LH, Zimmermann U. 1998. Simultaneous recording of xylem pressure and trans-root potential in roots of intact glycophytes using a novel xylem pressure probe technique. *Plant, Cell and Environment* **21,** 849–865.